Wear 486–487 (2021) 204103

Contents lists available at ScienceDirect

Wear

journal homepage: www.elsevier.com/locate/wear

Contact point lateral speed effects on contact strip wear in pantograph – catenary interaction for railway operations under 15 kV 16.67 Hz AC systems

Stefano Derosa [a,*], Petter Nåvik [a], Andrea Collina [b], Giuseppe Bucca [b], Anders Rønnquist [a]

[a] Department of Structural Engineering, Norwegian University of Science and Technology, Trondheim, Norway
[b] Department of Mechanical Engineering, Politecnico di Milano, Milan, Italy

ARTICLE INFO

Keywords:
Railway catenary systems
Pantograph-catenary sliding contact
Carbon strip wear model
Contact point lateral speed wear dependency

ABSTRACT

The design of a railway catenary is subject to multiple decisions regarding the geometry of the system. In particular, the horizontal geometry of the contact wire determines the evolution of the wear of the contact wire and contact strip over time. The horizontal geometry is obtained through the stagger, a lateral displacement of the contact wire at the supports. The value of the stagger, length of the span, curvature of the track, and train speed within the span determine the speed at which the contact point between the wire and the pantograph moves over the contact strip from side to side. A wider stagger corresponds to a larger area of the wear distribution over the contact strip. However, the speed at which the contact point moves over the strip is also important to the wear due to the sliding contact. Thus, the catenary design affects the contact strip wear through the lateral speed of the contact point. In this paper, a study of the lateral speed effects on contact strip wear is presented. The findings include a model of the lateral speed effect on the wear and a recommendation for a lower limit value for the lateral speed of 330 mm/s.

1. Introduction

Catenary infrastructure is a key component in electric railways. Trains rely on this complex system to harvest the required electric power to run, so a moving component onboard the train, i.e., the pantograph, must always remain in contact with a fixed component, i.e., the catenary. The quality of the contact has been greatly considered in pantograph-catenary interaction research [1]. A smaller variation in the forces at the contact point corresponds to a smoother sliding contact, which renders better working conditions. However, a significant consequence of this contact is the wear that affects the two parts involved: the contact wire and contact strip. Several parameters affect the wear behaviour, some of which directly result from design choices (e.g., the materials [2]) and others result from more complex dynamic phenomena [3] (e.g., the contact force [4]). The current intensity was studied in relation to the "current lubrication" effect [5] and the arcs for both AC [6] and DC [7] feeding systems. State-of-the-art wear investigations are based on laboratory experiments on specifically designed test rigs [8] due to the difficulty of obtaining significant results from field data. With a test rig, it is possible to explore different values of operational parameters and perform controlled, accurate measurements. However, due to the design of the test setup [9], the results of such tests are inherently more difficult to transfer to the field than those of other types of tests [10]. Nevertheless, it is possible to build wear models based on laboratory results. These models indicate the changes in level of wear when the operational parameters change. Although the values of wear are not comparable in absolute terms with those from the field, they remain valid for comparisons among different system configurations. The concept of wear maps [11] was first used to develop a wear model for both contact wire and contact strip [12]. A different approach was followed in Ref. [13], where a heuristic model of contact wire wear was built starting from considerations of the components that contributed to wear in Ref. [14] for a DC system. The same concept was applied in Ref. [15] to build two separate models of the wear in a copper-impregnated contact strip and a copper-silver contact wire under Norwegian operating conditions [16].

Current wear models mainly focus on the effects of the current and contact force, and some specific investigations have solely focused on contact strip materials (e.g., pure carbon [17], copper-impregnated carbon [18], iron base [19], and carbon composite [20]). However,

* Corresponding author.
E-mail address: stefano.derosa@ntnu.no (S. Derosa).

https://doi.org/10.1016/j.wear.2021.204103
Received 14 December 2020; Received in revised form 7 September 2021; Accepted 11 September 2021
Available online 13 September 2021

another parameter must be explored concerning wear, particularly for the contact strip: the stagger. The stagger is a catenary design parameter used to optimise the wear distribution of the contact strip. The stagger is realised by a lateral displacement of the contact wire with respect to the track centreline. The offset generally alternates from side to side at each catenary pole. This setup enables the wear to be distributed over a larger portion of the contact strip and avoids concentration on a single point. When designing a catenary system, several considerations must be made regarding the stagger [21]. More important than reducing the wear on the contact strip is optimising the catenary design to save as much material as possible. This requirement implies building longer spans, reducing the number of poles, and selecting a combination of span length and stagger that decreases the lateral forces generated by the contact wire at the supports, so that thinner structures can be designed. Thus, the stagger values may not always be as large (possibly up to 550 mm for 1950 mm pantographs, according to the EU TSI [22]) or as regular as would be considered in an ideal design. In particular situations such as around curves with a small radius, the stagger can be introduced on only one side, since the wire is pulled straight over a bent track. This design results in the contact point moving sideways on the contact strip, although the wire remains on the same side at all times. The variability from these design choices affects the way the contact point moves along the contact strip. Moreover, it is important to determine the position of the contact point on the contact strip and the speed at which the point moves laterally.

This study aims to analyse the effect of the contact point lateral speed on the contact strip wear. The starting point was the model developed for a copper-impregnated carbon contact strip operating under a 15 kV 16.67 Hz AC catenary system [15]. This model represents the wear as a function of the uplift force and current intensity. In this paper, a procedure to include the lateral speed as a variable of the model is presented. Furthermore, a lower limit for the lateral speed is recommended by considering the gradient of the wear model with respect to the speed.

A dedicated set of tests was designed to explore the wear behaviour at different contact point lateral speeds. These laboratory tests, which were performed with a contact couple identical to that in Ref. [15], are described in Chapter 2. In Chapter 3, the laboratory results are analysed to detect the eventual effect of the lateral speed on each component of the wear equation. Chapter 4 focuses on the creation of a function to describe the dependence of the contact strip wear on the lateral speed. Chapter 5 shows how this function is applied in the existing model and discusses the implications of this addition on wear modelling. Chapter 6 determines a limit for the lateral speed of the contact point, and chapter 7 presents the conclusions.

2. Laboratory tests

The required laboratory experiments were performed at Politecnico di Milano in Italy. A test rig designed to study the wear in pantograph-catenary interaction in the laboratories of the Department of Mechanical Engineering was used. For this particular study, experiments were performed with a constant current intensity of 300 A, a nominal uplift force of 60 N, a stagger value of ±200 mm and a train speed of 210 km/h. The values of the uplift force and current intensity refer to a single contact strip. The respective values must be modified accordingly for pantographs with multiple contact strips. The selected values of current intensity, uplift force and train speed correspond to typical values currently in use in the Norwegian Railway Network.

The stagger motion was reproduced via a linear actuator that operated on the contact strip in the direction perpendicular to the wire. To reproduce the train speed, a rotational motion was imposed on a fibreglass wheel with a 2.2 m radius, and a contact wire with a 100 mm^2 cross section was held on the edge via 36 elastic supports (Fig. 1(a)). In combination with the wheel rotation, an air duct provided an airflow with the speed that the contact couple would experience when running on a railway line. A complete and detailed description of the test rig is in Ref. [8].

The objective of the tests is to investigate the wear for different lateral speeds of the contact point. To fulfil this objective, the span length settings during sessions were changed to obtain different values of the lateral speed. The lateral speed ranged from 156 mm/s to 583 mm/s to simulate situations from very long to very short span lengths. Each span length was tested once to prioritise the investigation of different values of lateral speed over the repetition of the same test multiple times.

During the entire duration of each test, a set of force transducers placed on two sides of the contact strip measured the vertical and longitudinal forces. The ratio between the two forces was used to evaluate the friction coefficient between the contact strip and the wire. The current intensity and voltage were recorded to evaluate the electric resistance at the contact point [23] and the percentage of arcing during the test. Due to the operating conditions of the test rig, the measured percentage of arcing corresponds to the percentage of contact loss. One accelerometer was mounted in the middle of the contact strip along the vertical direction to gather information about the contact strip dynamics during the run. To reach a measurable level of wear, each run consisted of an equivalent travelled distance of 3000 km. Given the complexity of the test rig and selected values of the uplift force and train speed, the test duration was approximately three days for each configuration on average. The wear measurement was performed on the contact strip (Fig. 1(b)) by evaluating the mass before and after the test. A certified digital scale with an accuracy of 0.1 g was used, and the recorded value was the average of ten measurement repetitions. Finally, the loss of mass per kilometre was obtained by dividing the measured mass loss by the running distance.

Using the same criteria as those used in Ref. [15], the list of tests included a base case, which was required as a reference and used for comparison with other tests. The adoption of the base case is due to the differences in wear values between laboratory experiments and field measurements. These differences are due to factors such as the catenary elasticity, which does not have the same absolute value of a catenary in operation or the same evolution along a span. These conditions make a direct comparison of wear values unfeasible, although this leaves the possibility of comparing the results from different configurations in terms of the deviation from the base case. Considering the wear model assessed in Ref. [15] as a starting point, the base case selected in this work was similarly configured. Thus, in addition to the aforementioned values of the current intensity, uplift force, train speed and stagger, the selected span length was 60 m. The resulting lateral speed of the contact point was 389 mm/s. The unit of measurement for the lateral speed is mm/s due to the scale of the phenomenon, which is of a sensibly lower magnitude than the train speed.

Fig. 1. CuAg contact wire with a 100 mm^2 cross section (a) and a copper-impregnated carbon contact strip (b) used during the laboratory tests.

From the base case, different values of the span length were selected to cover possible values of the lateral speed of the contact point that may result from typical catenary design configurations. A shorter span length of 40 m was selected to obtain a lateral speed of 583 mm/s and investigate the domain of higher lateral speeds. On the other hand, low lateral speeds are known to be undesirable due to the increases in generated contact strip temperature, as noted by Delcey et al. in Ref. [24]. Hence, span length values of 80 m (292 mm/s), 120 m (194 mm/s) and 150 m (156 mm/s) were adopted to investigate a range of lower lateral speed values.

3. The wear model

Wear in pantograph-catenary interaction is a complex phenomenon. Although several factors contribute to the wear in the contact wire and contact strip, two main types of wear are identified [13]: mechanical and electrical. Mechanical wear occurs due to the friction between contact strip and contact wire, which acts against the sliding motion of one component over the other. Electrical wear is largely due to the Joule effect and consequently to the power dissipated as heat generated by the passage of electric current. Additionally, the presence of arcs that spark between pantograph and catenary whenever the contact is lost further contributes to the electrical wear.

The equation to account for these contributions, which was formulated in Ref. [13] and extended for the Norwegian conditions in Ref. [15], is as follows:

$$NWR = k_1 \left(\frac{1}{2}\cdot\left(1+\frac{I_c}{I_0}\right)\right)^{-\alpha} \cdot \left(\frac{F_m}{F_0}\right)^{\beta} \cdot \frac{F_m}{H} + k_2 \frac{R_c(F_m)\cdot I_c^2}{H\cdot V_0}(1-u) + k_3 u \frac{V_a I_c}{V_0 H_m \rho} \quad (1)$$

The normal wear rate (NWR) is defined as the volume of removed material in mm^3 per kilometre run. Table 1 lists all parameters and variables in Eq. (1).

The terms in the equation account for the three effects previously described. The first term represents mechanical wear, the second represents electrical wear in the form of the Joule effect, and the third represents electrical wear due to arcs. For the Joule effect term, the electrical contact resistance is described as follows [15]:

$$R_c = 0.3276 - 3.47\cdot 10^{-3}\cdot F \quad (2)$$

The validity of Eq. (2) is ensured in the force range of 30 N to 90 N.

Each term of Eq. (1) was investigated to detect its eventual dependence on the lateral speed of the contact point. The data recorded from the performed experiments were used to assess this dependence. Data from the current set of tests and previous test campaign in Ref. [15] were used in this section of the study. The tests from the previous campaign were named "Group 1", and the tests from the current campaign were named "Group 2". Importantly, the tests from Group 1 were performed by changing various parameters, i.e., the uplift force, current intensity and train speed, while the tests from Group 2 were performed by changing only the span length. Thus, the Group 1 data are outcomes from a larger investigation that provides a broader domain for the results. The specific Group 2 results for the lateral speed are placed within the Group 1 results for comparison. The entire experimental campaign, including both Group 1 and Group 2 tests, was performed with the intent of maximizing the domain of the results for all the studied parameters. This led to the inevitable choice of a selected number of values for each parameter. The considerations that follow are therefore based on the finite amount of results available for this study.

Table 1
List of the variables and parameters in Eq. (1).

Symbol	Description
k_1 [n/a]	Weight of the mechanical wear contribution
α [n/a]	Coefficient of the dependence of the mechanical wear on the current intensity
β [n/a]	Coefficient of the dependence of the mechanical wear on the force value
k_2 [n/a]	Weight of the electrical wear contribution
k_3 [n/a]	Weight of the arc wear contribution
F_m [N]	Contact force mean value
F_0 [N]	Contact force reference value
I_c [A]	Current intensity nominal value
I_0 [A]	Current intensity reference value
V_0 [m/s]	Sliding speed reference value
R_c [Ω]	Electrical contact resistance between contact strip and contact wire
u [%]	Percentage of contact loss
H [N/m^2]	Material hardness
H_m [J/kg]	Material latent heat of fusion
ρ [kg/m^3]	Material density
V_a [V]	Electrical arc voltage

3.1. Mechanical wear

To study the mechanical wear behaviour with the lateral speed of the contact point, the measured friction coefficient was considered. Fig. 2 shows the friction coefficients calculated from all tests performed with a contact couple made of a CuAg contact wire with a 100 mm^2 cross section and a copper-impregnated contact strip. The friction coefficients are plotted against the relative values of the lateral speed of the contact point. While all Group 2 tests were performed with an identical uplift force, Group 1 tests had different values of this force. In this figure, the results are divided into Group 1 with an uplift force of 60 N, Group 1 with an uplift force of 75 N and Group 2 with an uplift force of 60 N. No visible trend appears in the relations of the friction coefficients with the lateral speed and uplift force. The Group 2 results exhibit an almost constant behaviour for all assigned values of the lateral speed. Thus, the mechanical term can be excluded from the investigation of the lateral speed of the contact point.

3.2. Electrical wear – Joule effect

The possibility of a dependence of the second term of Eq. (1) on the lateral speed of the contact point was explored using the measured contact strip bulk temperature. Fig. 3 shows the results from Group 1 and Group 2 tests, which were divided by the current intensity, on which the Joule effect depends. Group 2 tests were performed with the identical current intensity of 300 A, while Group 1 tests were performed with increasing values of 300 A, 350 A and 400 A. If all results are considered,

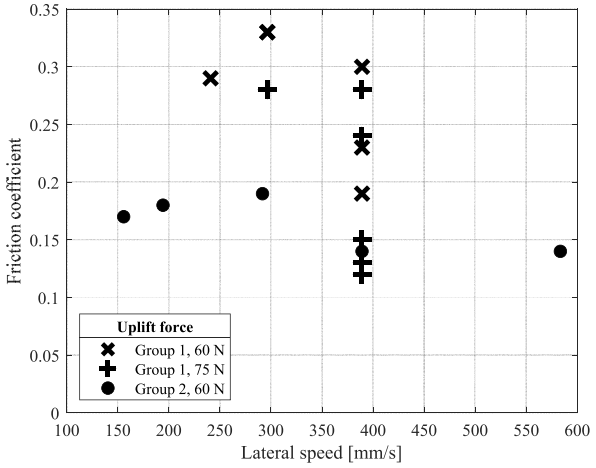

Fig. 2. Dependence of the friction coefficient on the lateral speed at the contact point; results from both Group 1 and Group 2 tests are shown with a further division over the applied uplift force for Group 1 tests.

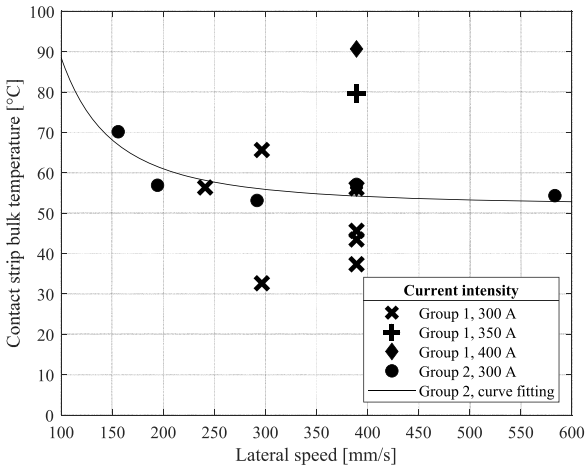

Fig. 3. Dependence of the contact strip core temperature on the lateral speed at the contact point; results from both Group 1 and Group 2 tests are shown, with a further division over the applied current intensity for the Group 1 tests. A curve fitting procedure was performed on the Group 2 points.

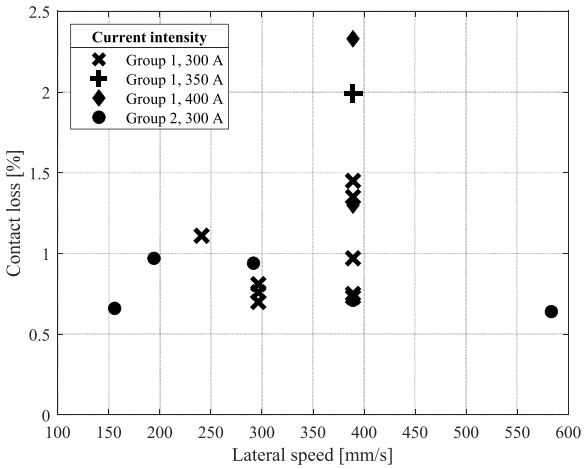

Fig. 4. Dependence of the contact loss on the lateral speed at the contact point; results from both Group 1 and Group 2 tests are shown, with a further division over the applied current intensity for the Group 1 tests.

no trend can be identified. However, with a focus on the results from Group 2, an inverse relationship between temperature and lateral speed is evident. Thus, it was decided to proceed only with Group 2 points, since they correspond to tests specifically designed to show possible trends with the lateral speed. Group 1 points also involve variations in several parameters, which leads to the possibility of including contributions from other effects. Nonetheless, Group 1 results show an increase in contact strip core temperature for increasing current intensity, which is consistent with the Joule effect. Then, a fitting procedure was performed for Group 2 results to highlight the possible trend of this wear component with respect to the lateral speed of the contact point.

3.3. Electrical wear – arcs

For the third and final term of Eq. (1), the analysis focuses on the contribution of the arcs to the overall wear. During the tests, voltage values were recorded and used to detect whenever the contact between wire and strip was lost, which indicated that an arc was generated. The choice of the voltage signal as an arc detector was due to the increase in voltage whenever the electric resistance at the contact point increased due to the contact loss. The time at which the voltage signal exceeded a set threshold was related to the total measurement time to evaluate the parameter of the percentage of contact loss. Higher values of the percentage of contact loss result in higher contributions of the arcs to the overall wear. Fig. 4 shows the contact loss values for all performed tests. Since the arc term is associated with electrical wear, the results are again presented from the point of view of the current intensity. Similar to the mechanical wear case, it was not possible to define a trend for the selected parameters when plotted against the lateral speed. Thus, the arc term was also excluded from the lateral speed analysis, and only the inverse relationship with the train speed remained. This relation is valid because higher train speeds were shown in Ref. [25] to be beneficial for reducing the duration of arcs, which decreased the damage that they could cause to the contact wire and contact strip.

4. Wear behaviour vs lateral speed of the contact point

Following the analysis of every term of Eq. (1), a coefficient for the second term (electrical wear, Joule effect) was added to account for lateral speed effects. Eq. (3) shows the updated version of the NWR equation, where $k_4(v_l)$ indicates that a coefficient function of lateral speed is included.

$$NWR = k_1\left(\frac{1}{2}\cdot\left(1+\frac{I_c}{I_0}\right)\right)^{-\alpha}\cdot\left(\frac{F_m}{F_0}\right)^{\beta}\cdot\frac{F_m}{H}+k_4(v_l)k_2\frac{R_c(F_m)\cdot I_c^2}{H\cdot V_0}(1-u) + k_3 u\frac{V_a I_c}{V_0 H_m \rho} \quad (3)$$

In this section, the procedure to define this new coefficient is explained, starting from measured NWR results and by applying a necessary correction that accounts for the test rig design.

4.1. Measured contact strip wear results

The starting point to establish a coefficient function of the lateral speed was the set of Group 2 test results. Fig. 5 shows the wear values, which were measured in worn volume per kilometre run and plotted against the corresponding values of lateral speed. Given the assumption

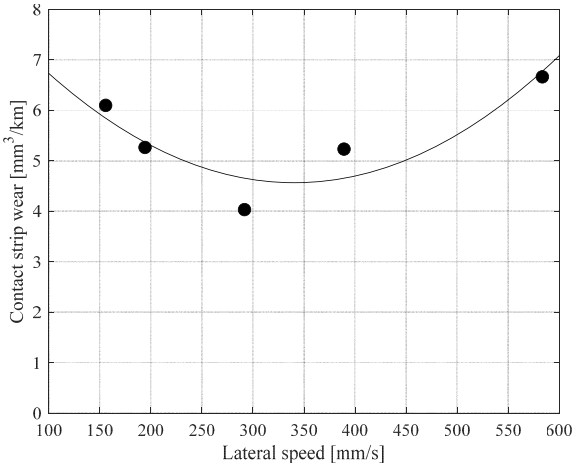

Fig. 5. NWR results from the laboratory tests performed with variable span length (Group 2); a second-degree polynomial fitting curve is plotted to show a plausible trend for the measured points. Measured data for the contact strip have an accuracy of 1%.

in section 3, the behaviour of the NWR points against the lateral speed of the contact point was expected to be similar to that of the contact strip temperature in Fig. 3. However, it shows that this assumption holds only for low lateral speed values and is not valid for higher speeds. This discrepancy occurs due to the design of the test rig. In a railway catenary, the stagger is realised by displacing the contact wire on the horizontal plane. Meanwhile, the pantograph maintains its position with respect to the track centreline. In the test rig, the opposite occurs. The contact wire, which is fastened to the 2.2-m-radius fibreglass wheel, maintains its position with respect to the hypothetical track centreline, while the contact strip moves in the direction perpendicular to the wire to realise the same effect as the stagger. This arrangement is very convenient in terms of machine operation, since it enables the movement of the smaller component of the contact couple, i.e., the contact strip. However, when the lateral speed of the contact point increases, a significant lateral dynamic is added to the system at the frequency that is twice the span passing frequency. This distortion of the dynamic conditions at which the system operates affected the results. Thus, a more in-depth analysis was performed on the lateral motion associated with the contact strip. In the next section, the procedure for this specific study is explained.

4.2. Contact strip lateral dynamic

To study the effects of the test rig design on the contact strip wear results, a dedicated set of runs was performed. The aim was to harvest as much information as possible on the contact strip dynamic over a wide range of lateral speeds of the contact point. For this specific campaign, three additional accelerometers were added to the contact strip setup. Two of them were mounted at the two ends of the contact strip along the vertical direction, and one was placed on the right side of the contact strip in the lateral direction. Different values of lateral speed were reached in two ways: maintaining a constant span length while varying the train speed and maintaining a constant train speed while varying the span length. A frequency analysis was conducted on the content of the added dynamic response. For each of the 27 tested speed steps, the corresponding span passing frequency value and Fourier transform of the lateral acceleration were evaluated. Then, the magnitude of the Fourier transform for the frequency that was twice the span passing frequency was extracted. Fig. 6 shows these magnitude values versus the respective lateral speed. The points marked with X coincide with the train speed step tests, while the points marked with a dot are the results of the span length step tests. The energy content introduced in the lateral acceleration signal by the imposed contact strip lateral motion notably increases above a lateral speed of approximately 300 mm/s. From this observation, the NWR values were corrected to create a curve that accounted for the added dynamic and to scale the wear points accordingly.

4.3. Dynamic correction of the wear results

To perform the required correction, information from the data points in Fig. 6 was used. A curve was built by fitting these points with an exponential type of function. However, another step was performed before the curve was used to scale the NWR results. The curve was to provide a correction for those points where an additional dynamic was introduced. According to the observations in section 4.2, up to a lateral speed of approximately 300 mm/s, the situation had no or only a small additional dynamic. For higher speeds, the curve notably increased. This behaviour was replicated with a curve that provided unit values for the contact point lateral speed values that were unaffected by the additional dynamic and grew accordingly for the affected speed values. The resulting correction curve is presented in the bottom plot of Fig. 7. The upper plot of Fig. 7 includes both original wear points and corrected points to show how the correction leaves the points at low speeds unaltered, while it changes the points at higher speeds. A polynomial curve of degree -2 was also fitted to the corrected data and provided a function that represented the behaviour of the wear for the considered range of lateral speed values. The last step was to normalise the curve in Fig. 7 using the base case value as a scaling factor. Thus, the NWR value for the base case remains the same after the addition of coefficient $k_4(v_l)$ to Eq. (1). Fig. 8 shows the normalisation result, where coefficient $k_4(v_l)$ is presented as a function of the lateral speed as follows:

$$k_4(v_l) = 0.21 \cdot \frac{v_{l_0}^2}{v_l^2} + 0.79 \tag{4}$$

Because the curve is a polynomial of degree -2, the form of equation k_4 must be changed to re-establish its correctness for the unit of measurement. Thus, the square of the base case lateral speed was added to the first term, and the corresponding coefficient was scaled accordingly.

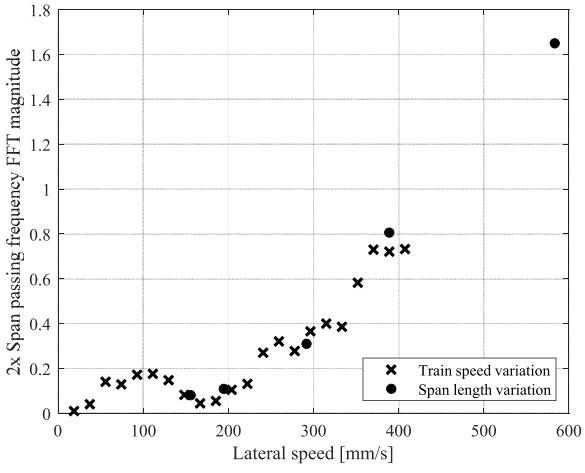

Fig. 6. FFT magnitude at the frequency corresponding to twice the span passing frequency for different lateral speeds of the contact point; the values of the lateral speed were reached by either varying the train speed (**X**) or the span length (●).

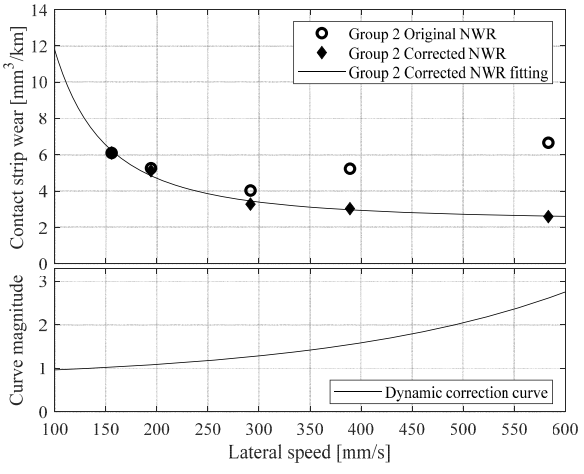

Fig. 7. Top plot: Contact strip wear data before and after correction, with the curve fitting performed on the latter. Bottom plot: Curve used for the correction of the introduced dynamic effects. Measured data for the contact strip have an accuracy of 1%.

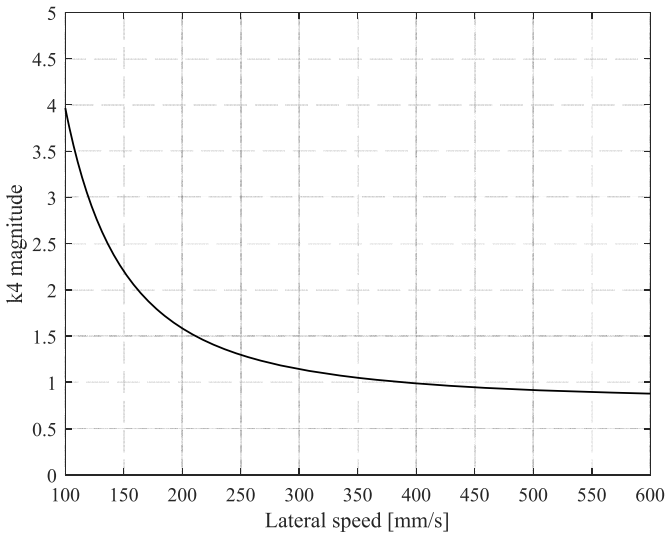

Fig. 8. k4 coefficient as a function of the lateral speed of the contact point.

5. Contact strip wear model extension

Once the k_4 coefficient was determined, it was possible to update the contact strip wear model with the updated contact point lateral speed variable as follows:

$$NWR = 0.02\left(\frac{F_m}{F_0}\right)^{-0.45}\cdot\frac{F_m}{H}+0.015\left(0.21\cdot\frac{v_{l0}^2}{v_l^2}+0.79\right)\frac{R_c(F_m)\cdot I_c^2}{H\cdot V_0}(1-u) + 9.692u\frac{V_a I_c}{V_0 H_m \rho} \tag{5}$$

Eq. (5) shows the resulting model with the addition of the coefficient values from Ref. [15]. The wear model can now represent the dependence of the contact strip wear on the parameters of the uplift force, current intensity and lateral speed of the contact point. Fig. 9 shows the trend of the model with respect to the values of the lateral speed of the contact point from 100 mm/s to 600 mm/s. Three plots are presented for increasing values of the uplift force from 45 N to 75 N, and the base case value of 60 N is in the middle. For each plot, three values of current intensity were selected: 300 A, 350 A and 400 A. According to the findings from Ref. [15], an increase in current intensity increases the contact strip wear, while an increase in uplift force decreases the wear. Regarding the lateral speed of the contact point, the behaviour follows a similar trend to that observed for the contact strip bulk temperature in Fig. 3. At low speed values, the wear appears to be notably higher than that in the range of faster contact point lateral movement. Furthermore, after a speed value of approximately 300 mm/s has been exceeded, the wear value behaviour appears to become stable. Fig. 10 helps to understand the contribution of each term to the total wear. The plot refers to the base case and features an uplift force of 60 N and a current intensity of 300 A. The mechanical and arc components, which were excluded by the lateral speed dependency analysis, show a constant behaviour throughout the entire contact point lateral speed domain. The contribution is only a small fraction of the total wear. A higher contribution, as noted in Ref. [15], comes from the electrical term related to the Joule effect. This phenomenon is particularly valid at low lateral speeds, where a larger temperature increase was detected in the contact strip core.

6. Contact point lateral speed limit

From the analysis of the base case wear, observations were made to provide suggestions for a lateral speed limit. Section 2 mentioned that the results from this type of test are not directly applicable to a real case, and it is preferable to work on comparisons for variations in operating conditions. Thus, a decision regarding a lateral speed limit cannot be assessed based on the absolute values of the wear. A better approach is to study the rate of change in wear value with increasing lateral speed. Fig. 11 shows the trend of the variation in wear values for the base case,

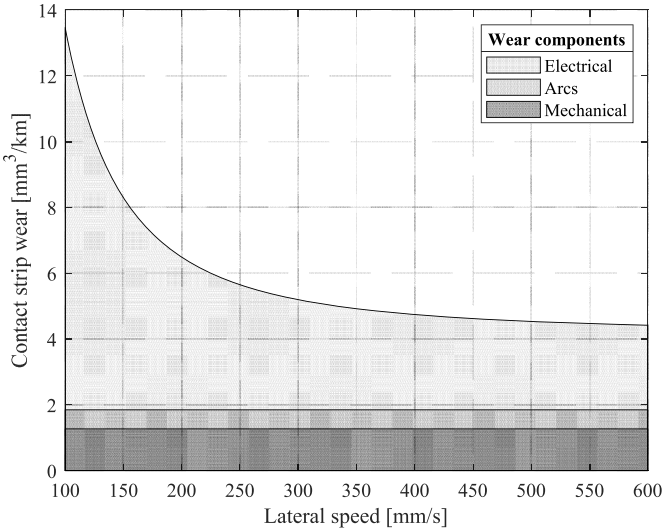

Fig. 10. NWR model for the prediction of the contact strip wear as a function of the lateral speed, divided by three types of components: mechanical, electrical and arcs. The base case with an uplift force of 60 N and a current intensity of 300 A is represented here.

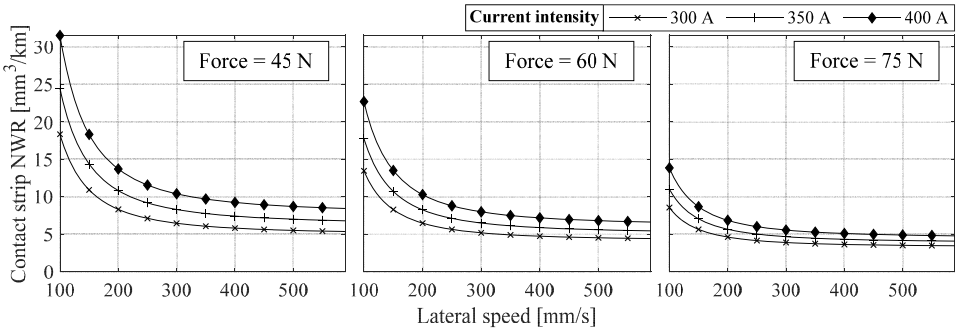

Fig. 9. NWR model for the prediction of the contact strip wear as a function of the lateral speed. Three different uplift forces of 45 N, 60 N and 75 N were selected; for each force, current intensities of 300 A, 350 A and 400 A are represented.

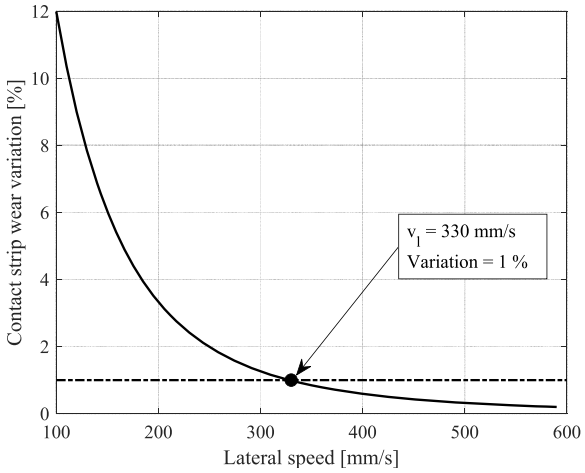

Fig. 11. NWR model gradient for the base case (uplift force of 60 N, current intensity of 300 A); the threshold of the lateral speed is set at 330 mm/s, where the variation meets the 1% value, marked by the dash-dotted line.

which was evaluated over speed steps of 10 mm/s. Every step at a low speed value gives an important reduction in wear, while for higher speed values the difference becomes less noticeable. The threshold was set at the point where the difference between two steps became less than 1%. The corresponding contact point lateral speed value of 330 mm/s was set as a possible lower limit for the lateral speed of the contact point as a result of the span length, stagger and train speed.

To understand the magnitude of this limit value, examples of the lateral speed are provided in Fig. 12. In the top row, three examples from Norwegian railways are shown. The left plot refers to the newest line designed exclusively for passenger service with an operating speed of 210 km/h. The plot shows the lateral speeds evaluated for a span on a straight section (solid line) and for a span on a curved track (dashed line) with the stagger positioned on opposite sides of the track at the two ends of the span. The values of lateral speed are always above the set limit, which is represented by a dash-dotted line. A different situation occurs when a winding railway such as Dovrebanen is considered. For this line, the traffic is mixed, with both freight and passenger trains running on it. Although the line was identical, different operating conditions with speeds of 130 km/h for passenger trains and 90 km/h for freight trains lead to different plots of the lateral speed. For freight traffic, the lateral speed along the straight track is exceptionally close to the limit, which suggests more careful monitoring of the pantographs in use on locomotives assigned to freight service. Another aspect to consider for this line is the presence of a curved track with the contact wire designed to have the stagger on the same side of the track at both ends of the span. This is a common case for tight curves, but it makes the lateral speed decrease to zero when the wire and track are parallel. Although the limit value is crossed, the short time in which this occurs does not constitute an issue. However, particular care should be taken when this arrangement occurs multiple times on the same line stretch. In the bottom row, two examples of high-speed passenger lines are presented, both of which have an operating speed of 300 km/h. In this case, on a straight track, the lateral speed values are well above the limit, although a smaller stagger value is adopted on longer spans. Curved tracks for high-speed lines are designed with very wide radii and behave similarly to straight tracks; therefore, they were not included in the plots. An additional critical point characterised by a low lateral speed of the contact point is the stations. At the start, trains are slow and draw more current from the line. This combination of factors contributes to increasing the wear in the contact strips.

To generate the plots included in Fig. 12, data regarding span length, stagger and curve radius were gathered for the different lines. Table 2 shows the values chosen as an example for each case.

In conclusion, freight operations are more at risk of crossing the lateral speed limit, mainly due to their lower speed. Furthermore, heavier trains are more likely to draw more power from the catenary, which translates into higher current intensity values and higher wear for a system at a constant voltage (Fig. 9). Meanwhile, for passenger services, the situation is usually better, with lateral speed values well above the limit, and the exception is only limited sections on tight curves. The

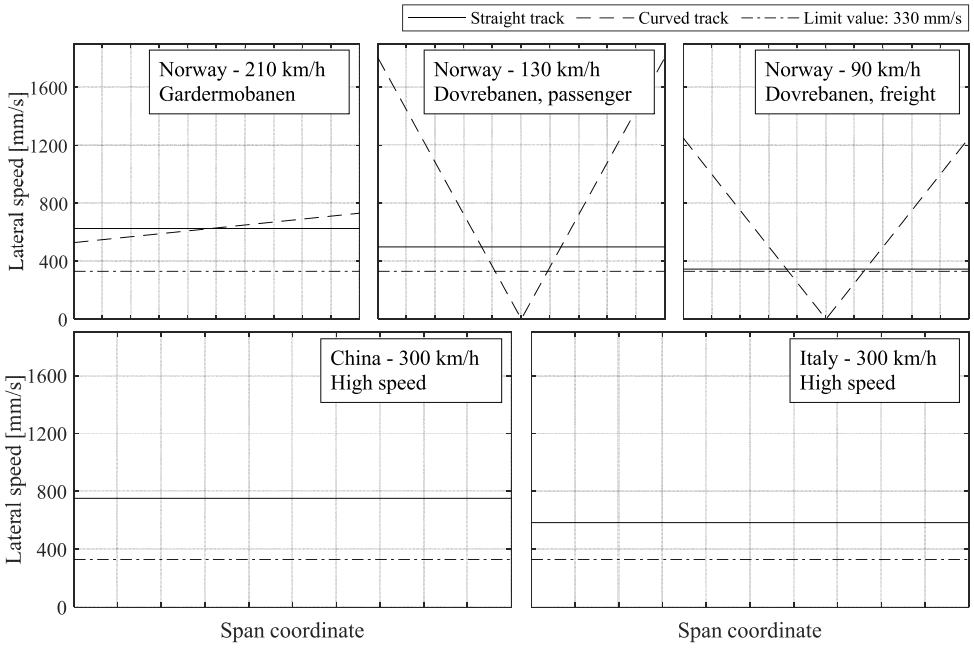

Fig. 12. Contact point lateral speed examples for various operating conditions. The top row refers to two lines in Norway for fast passenger service (Gardermobanen) and mixed passenger/freight traffic with different operating speeds (Dovrebanen). The bottom row refers to two high-speed lines in China (left) and Italy (right). For all cases, the lateral speed limit is plotted with a dash-dotted line.

Table 2
List of the parameters used to evaluate the contact point lateral speed values presented in Fig. 12.

Country	Line	Service	Speed	Span length	Track radius	Stagger
			km/h	m	m	mm
Norway	Gardermobanen	Passenger	210	56.0	—	+300, -300
Norway	Gardermobanen	Passenger	210	55.6	15984	+300, -300
Norway	Dovrebanen	Passenger	130	58.0	—	+400, -400
Norway	Dovrebanen	Passenger	130	40.0	400	-400, -400
Norway	Dovrebanen	Freight	90	58.0	—	+400, -400
Norway	Dovrebanen	Freight	90	40.0	400	-400, -400
China	High-speed	Passenger	300	55.4	—	+250, -250
Italy	High-speed	Passenger	300	57	—	+250, -250

differences caused by the operating speed even on the same railway line show the importance of considering both the maximum allowed speed and the intended operating speed for each type of service that will use the line in the design stage.

7. Conclusions

This paper addresses wear in pantograph-catenary interaction in electric railways. In particular, the focus is on the lateral speed of the contact point between the pantograph and the catenary. This speed is found to affect the wear in the contact strip. The study investigates this effect by addressing the wear modelling by components.

The findings can be summarised as follows:

- The lateral speed does not affect the mechanical wear and electrical wear associated with the arcs. However, it affects the electrical term associated with the Joule effect. A procedure to add this effect to the existing wear model is presented, and the new model with the included lateral speed variable is displayed. The model, which could provide the wear of the contact strip as a function of the uplift force and current intensity, can now provide the wear as a function of the lateral speed. This update enables to link the wear to the design parameters that determine the lateral speed, such as the span length, stagger and train speed.
- A threshold value of 330 mm/s was estimated for the lateral speed of the contact point. This threshold enables one to set a new control parameter when considering the span length, stagger and train speed in the design of catenary infrastructure. In particular, this aspect underlines the importance of the combination of these three parameters, which were shown to greatly affect the wear behaviour below the set threshold.

CRediT authorship contribution statement

Stefano Derosa: Conceptualization, Methodology, Software, Validation, Formal analysis, Investigation, Data curation, Writing – original draft, Visualization. **Petter Nåvik:** Conceptualization, Methodology, Resources, Writing – review & editing. **Andrea Collina:** Methodology, Resources, Writing – review & editing. **Giuseppe Bucca:** Conceptualization, Methodology, Software, Validation, Investigation, Data curation, Writing – review & editing, Visualization. **Anders Rønnquist:** Methodology, Validation, Resources, Writing – review & editing, Supervision, Project administration, Funding acquisition.

Declaration of competing interest

The authors declare that they have no known competing financial interests or personal relationships that could have appeared to influence the work reported in this paper.

Acknowledgements

The authors are grateful to the Norwegian Railway Directorate for funding this research.

References

[1] S. Bruni, G. Bucca, M. Carnevale, A. Collina, A. Facchinetti, Pantograph–catenary interaction: recent achievements and future research challenges, Int J Rail Transp (2017) 1–26, https://doi.org/10.1080/23248378.2017.1400156, 00.
[2] H. Borgwardt, Verschleiß Verhalten des Fahrdraht der Oberleitung, Elektrische Bahnen 87 (1989) 287–295.
[3] P. Nåvik, A. Rønnquist, S. Stichel, The use of dynamic response to evaluate and improve the optimization of existing soft railway catenary systems for higher speeds, Proc. Inst. Mech. Eng. - Part F J. Rail Rapid Transit 230 (2015) 1388–1396, https://doi.org/10.1177/0954409715605140.
[4] D. Klapas, F.A. Benson, R. Hackam, P.R. Evison, Wear in simulated railway overhead current collection systems, Wear 126 (1988) 167–190, https://doi.org/10.1016/0043-1648(88)90136-6.
[5] A. Senouci, J. Frene, H. Zaidi, Wear mechanism in graphite-copper electrical sliding contact, Wear 225–229 (1999) 949–953, https://doi.org/10.1016/S0043-1648(98)00412-8.
[6] G. Bucca, A. Collina, E. Tanzi, Experimental analysis of the influence of the electrical arc on the wear rate of contact strip and contact wire in a.c. System, Int J Mech Control 18 (2017) 449–456, https://doi.org/10.1007/978-3-319-48375-7_48.
[7] S. Kubo, K. Kato, Effect of arc discharge on wear rate of Cu-impregnated carbon strip in unlubricated sliding against Cu trolley under electric current, Wear 216 (1998) 172–178, https://doi.org/10.1016/S0043-1648(97)00184-1.
[8] M. Bocciolone, A. Collina, G. Bucca, F. Mapelli, A test rig for the comparative evaluation of the performance of collector strips, Proc Railw Eng Conf (2004) 1–11.
[9] K. Becker, A. Rukwied, W. Zweig, U. Resch, Simulation of the wear behaviour of high-speed over-head current collection systems, Trans Built Environ 17 (1996) 281–290.
[10] S. Bruni, G. Bucca, A. Collina, A. Facchinetti, S. Melzi, Pantograph-catenary dynamic interaction in the medium-high frequency range, Veh. Syst. Dyn. 41 (2004) 697–706.
[11] S.C. Lim, M.F. Ashby, Wear-Mechanism maps, Acta Metall. 35 (1987) 1–24, https://doi.org/10.1016/0001-6160(87)90209-4.
[12] G. Bucca, A. Collina, A procedure for the wear prediction of collector strip and contact wire in pantograph-catenary system, Wear 266 (2009) 46–59, https://doi.org/10.1016/j.wear.2008.05.006.
[13] G. Bucca, A. Collina, Electromechanical interaction between carbon-based pantograph strip and copper contact wire: a heuristic wear model, Tribol. Int. 92 (2015) 47–56, https://doi.org/10.1016/j.triboint.2015.05.019.
[14] A. Collina, S. Melzi, A. Facchinetti, On the prediction of wear of contact wire in OHE lines: a proposed model, Veh. Syst. Dyn. 37 (2002) 579–592, https://doi.org/10.1080/00423114.2002.11666264.
[15] S. Derosa, P. Nåvik, A. Collina, G. Bucca, A. Rønnquist, A heuristic wear model for the contact strip and contact wire in pantograph – catenary interaction for railway operations under 15 kV 16.67 Hz AC systems, Wear 457 (2020) 203401, https://doi.org/10.1016/j.wear.2020.203401.
[16] A. Rønnquist, P. Nåvik, Dynamic assessment of existing soft catenary systems using modal analysis to explore higher train velocities: a case study of a Norwegian contact line system, Veh. Syst. Dyn. 53 (2015) 756–774, https://doi.org/10.1080/00423114.2015.1013040.
[17] T. Ding, G.X. Chen, X. Wang, M.H. Zhu, W.H. Zhang, W.X. Zhou, Friction and wear behavior of pure carbon strip sliding against copper contact wire under AC passage at high speeds, Tribol. Int. 44 (2011) 437–444, https://doi.org/10.1016/j.triboint.2010.11.022.
[18] S. Kubo, K. Kato, Effect of arc discharge on the wear rate and wear mode transition of a copper-impregnated metallized carbon contact strip sliding against a copper disk, Tribol. Int. 32 (1999) 367–378, https://doi.org/10.1016/S0301-679X(99)00062-6.
[19] H. Nagasawa, K. Kato, Wear mechanism of copper alloy wire sliding against iron-base strip under electric current, Wear 216 (1998) 179–183, https://doi.org/10.1016/S0043-1648(97)00162-2.
[20] Y. Kubota, S. Nagasaka, T. Miyauchi, C. Yamashita, H. Kakishima, Sliding wear behavior of copper alloy impregnated C/C composites under an electrical current, Wear 302 (2013) 1492–1498, https://doi.org/10.1016/j.wear.2012.11.029.

[21] F. Kiessling, R. Puschmann, A. Schmieder, E. Schneider, in: Contact Lines for Electric Railways, third ed., Publicis, Erlangen, 2018.
[22] Commission Regulation (EU), No 1301/2014 on the Technical Specifications for Interoperability Relating to the "Energy" Subsystem of the Rail System in the Union, 2014.
[23] G. Bucca, A. Collina, R. Manigrasso, F. Mapelli, D. Tarsitano, Analysis of electrical interferences related to the current collection quality in pantograph-catenary interaction, Proc. Inst. Mech. Eng. - Part F J. Rail Rapid Transit 225 (2011) 483–499, https://doi.org/10.1177/0954409710396786.
[24] N. Delcey, P. Baucour, D. Chamagne, G. Wimmer, G. Bucca, N. Bruyere, et al., Analysis of the thermal variations in a moving pantograph strip using an electro-thermal simulation tool and validating by experimental tests, Proc. Inst. Mech. Eng. - Part F J. Rail Rapid Transit 234 (2020) 859–868, https://doi.org/10.1177/0954409719877341.
[25] D. Bormann, S. Midya, R. Thottappillil, DC components in pantograph arcing: mechanisms and influence of various parameters, Proc 18th Int Zurich Symp Electromagn Compat EMC 369–72 (2007), https://doi.org/10.1109/EMCZUR.2007.4388272.